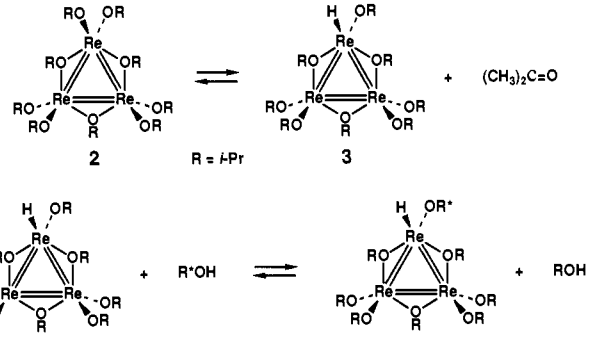

direction, equilibrium 3 represents β-hydrogen activation at a terminal isopropoxide ligand of **2** and accounts for the presence of **3** and acetone in solution. Equilibrium 4 is an exchange process between the unique terminal isopropoxide ligand of **3** and free isopropyl alcohol; thus, 4 accounts for the observed broadening in the resonances of one isopropoxide ligand of **3** and isopropyl alcohol.

Further evidence for the assigned structure of **3** and equilibria 3 and 4 comes from the following NMR experiments: (i) Proton NMR resonances arising from **3** grow in intensity relative to those from **2** at temperatures above room temperature, whereas at lower temperatures the concentration of **3** decreases relative to **2**. The spectral changes are fully reversible, consistent with eq 3. (ii) Addition of acetone to a benzene-d_6 solution of **2** results in the complete disappearance of resonances arising from **3**. This is consistent with a shift of eq 3 to the left. (iii) Addition of an excess of pyridine-d_5 (≈100 equiv) to a benzene-d_6 solution of **2** gives, by ^{1}H NMR, a mixture of free acetone, free isopropyl alcohol, and a pyridine adduct of **3** (**3-py**). On the basis of the NMR spectrum, **3-py**, like **3**, has virtual mirror symmetry. Assignable to **3-py** are a hydride resonance at δ −1.97, five sharp OC(*H*)Me$_2$ septets in the ratio of 2:2:2:1:1, and eight sharp methyl doublets of equal intensity. The free isopropyl alcohol resonances are also sharp. These observations are consistent with 3 and 4 in that pyridine is expected to coordinate to the sterically accessible ReH(OR) site, thereby blocking the position and shutting down acetone reinsertion (shifting 3 to the right) and isopropyl alcohol–isopropoxide exchange. (iv) Addition of an excess of isopropyl alcohol-d_8 (≈100 equiv) to a benzene-d_6 solution of **2** results (<30 min) in the complete disappearance of proton resonances arising from the terminal alkoxide positions of **2** and **3** as well as the hydride resonance of **3**. This indicates that isopropyl alcohol–isopropoxide exchange involves only terminal alkoxides and that bridge-terminal alkoxide exchange in **2** and **3** is slow compared to 3 and 4. Moreover, because resonances from only one alkoxide are broad under conditions of fast exchange (e.g., at 23 °C, Figure 1), the rapidly exchanging isopropoxide must be the one indicated in eq 4. Presumably, rapid isopropyl alcohol–isopropoxide exchange occurs only for this alkoxide because there is less steric crowding at this site.[7] (v) Addition of an excess of acetone-d_6 (≈100 equiv) to a benzene-d_6 solution of **2** gives, after 1 h, a ^{1}H NMR spectrum that is consistent with $Re_3(\mu\text{-}OC(H)(CH_3)_2)_3(OC(H)(CD_3)_2)_6$ and $(CH_3)_2C{=}O$ in solution.[8] Two conclusions can be drawn from this result: The source of the hydride ligand in **3** cannot be a bridging alkoxide ligand, and, because deuterium is not incorporated into the methine position of the terminal isopropoxides of **2**, the hydride ligand in **3** must originate from the β-hydrogens of the terminal alkoxides of **2**.

In summary, we have synthesized the first homoleptic rhenium alkoxide complex and have established that it undergoes reversible alkoxide β-hydrogen elimination. Further mechanistic and synthetic studies, including the isolation of **3** and **3-py**, are in progress.

Acknowledgment is made to the donors of the Petroleum Research Fund, administered by the American Chemical Society, for the support of this research.

(7) A referee suggested that the ReH(OR) metal center is also more Lewis acidic than the Re(OR)$_2$ centers because it has one less π-donor ligand. Greater Lewis acidity would also account for the enhanced exchange rate.

(8) Spectra recorded over 48 h indicate that more extensive deuterium scrambling occurs at longer reaction times.

Supplementary Material Available: Tables of crystal data, atomic coordinates, and thermal parameters and a ball-and-stick plot of **2** (7 pages); table of observed and calculated structure factors (10 pages). Ordering information is given on any current masthead page.

Two-Dimensional Solid-State NMR of a Captive Intermediate: Structure of the Radical Centers in 3,4-Dimethylenethiophene

Kurt W. Zilm,* Ronald A. Merrill, Gretchen G. Webb, Marc M. Greenberg, and Jerome A. Berson

Department of Chemistry, Yale University
225 Prospect Street, New Haven, Connecticut 06520
Received June 8, 1987

Matrix isolation studies are important for furthering our understanding of reaction mechanisms and provide an experimental means of checking theoretical predictions of novel molecular geometries. However, no direct methods have yet been developed for experimentally determining the structures of matrix-isolated species. In this paper we report on a two-dimensional (2D) solid-state NMR technique which provides a convenient method for determining the structures of matrix-isolated molecules and for spectroscopically assigning their ^{13}C CPMAS spectra. This technique has been used in the first direct structure determination of a captive intermediate, 3,4-dimethylenethiophene, **1a**. Both the H–C–H angle and C–H distances have been determined for the radical centers in **1a**, and the results confirm the assignment[1] of the singlet biradical structure to this intermediate.

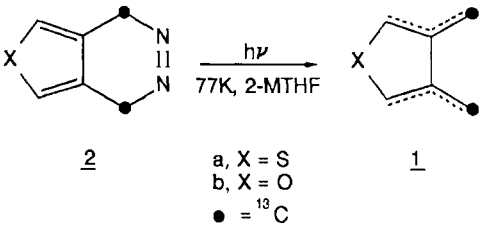

Previous studies[2] have demonstrated the feasibility of using dipolar coupled powder NMR spectra for measuring bond lengths in small molecules trapped in rare gas matrices. The principal difficulty in using this method to study more complex captive intermediates is spectral overlap of the dipolar coupled powder patterns.[2c] The combination[3,4] of CPMAS methods with 2D separated local field (MASSLF) spectroscopy[5] circumvents this difficulty by separating the proton dipolar coupled spectra for each carbon on the basis of their isotropic chemical shifts. For each line in the ^{13}C CPMAS spectrum a dipolar coupled sideband pattern is generated by taking a slice in the 2D MASSLF spectrum along the first frequency dimension. The envelope of these

(1) (a) Zilm, K. W.; Merrill, R. A.; Greenberg, M. M.; Berson, J. A. *J. Am. Chem. Soc.* **1987**, *109*, 1567–1569. (b) Stone, K. J.; Greenberg, M. M.; Goodman, J. L.; Peters, K. S.; Berson, J. A. *J. Am. Chem. Soc.* **1986**, *108*, 8088–8089. (c) Du, P.; Hrovat, D. A.; Borden, W. T. *J. Am. Chem. Soc.* **1986**, *108*, 8086–8087. (d) Lahti, P. M.; Rossi, A. R.; Berson, J. A. *J. Am. Chem. Soc.* **1985**, *107*, 2273–2280.

(2) (a) Kohl, J. E.; Semack, M. G.; White, D. *J. Chem. Phys.* **1978**, *69*, 5378–5385. (b) Zilm, K. W.; Grant, D. M. *J. Am. Chem. Soc.* **1981**, *103*, 2913–2922. (c) Orendt, A. M.; Arnold, B. R.; Radziszewski, J. G.; Facelli, J. C.; Malsch, K. D.; Strub, H.; Grant, D. M.; Michl, J. *J. Am. Chem. Soc.* **1988**, *110*, 2648–2650.

(3) (a) Munowitz, M. G.; Griffin, R. G.; Bodenhausen, G.; Huang, T. H. *J. Am. Chem. Soc.* **1981**, *103*, 2529–2533. (b) Munowitz, M. G.; Griffin, R. G. *J. Chem. Phys.* **1982**, *76*, 2848–2858.

(4) (a) Schaefer, J.; McKay, R. A.; Stejskal, E. O.; Dixon, W. T. *J. Magn. Reson.* **1983**, *52*, 123–129. (b) Schaefer, J.; Sefcik, M. D.; Stejskal, E. O.; McKay, R. A.; Dixon, W. T.; Cais, R. E. *Macromolecules* **1984**, *17*, 1107–1118.

(5) (a) Hester, R. K.; Ackerman, J. L.; Neff, B. L.; Waugh, J. S. *Phys. Rev. Lett.* **1976**, *36*, 1081–1083. (b) Stoll, M. E.; Vega, A. J.; Vaughan, R. W. *J. Chem. Phys.* **1976**, *65*, 4093–4098.

0002-7863/89/1511-1533$01.50/0

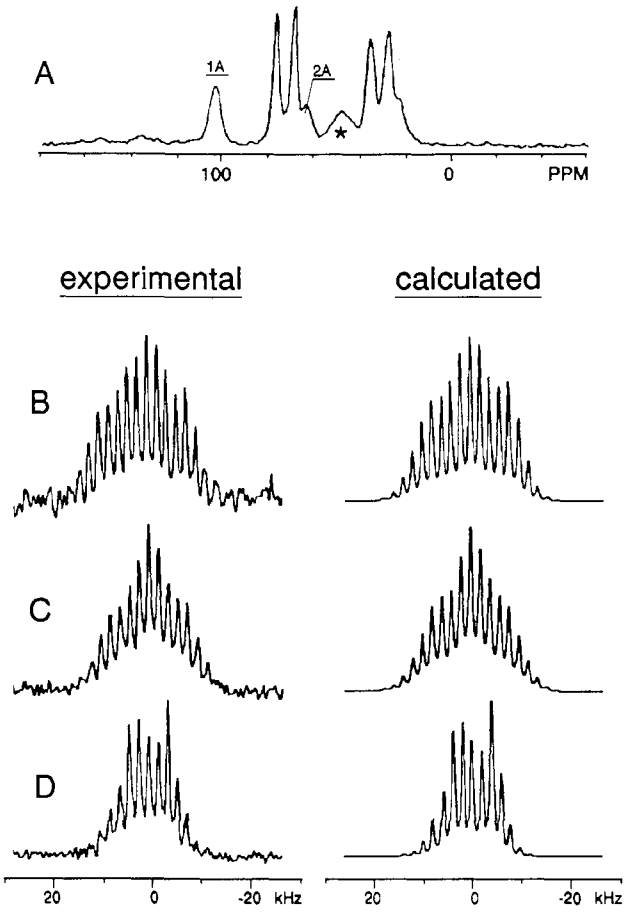

Figure 1. (A) ^{13}C CPMAS spectrum at 77 K for a sample of **2a** in 2-MTHF after 3 h of photolysis. The unlabeled lines are for the 2-MTHF matrix. Resonances assigned to the ^{13}C enriched centers in **1a** and **2a** are indicated. * marks a line due to the hydrazo precursor of **2a**. Experimental MASSLF patterns are shown in B–D: (B) pattern for the 105 ppm peak in A, (C) pattern for a methylene, and (D) for the methine in 2-MTHF. Simulations which are essentially identical with the experimental spectra are shown to their immediate right. The r_{CH} used in these simulations was 1.09 Å for the 2-MTHF and 1.08 Å for the labeled centers in **1a**. In B the H–C–H angle was set to 120°. The shift tensor used here is oriented with σ_{33} perpendicular to the H–C–H plane and σ_{22} in the H–C–H plane along the bisector of the H–C–H angle. The principal values of the shift tensor used in this simulation are σ_{11} = 145 ppm, σ_{22} = 105 ppm, and σ_{33} = 65 ppm.

spinning sideband patterns closely mimics the shape of static dipolar coupled powder spectra and accurately determines the size, number, and relative orientations of the dipolar couplings each ^{13}C nucleus experiences. Versions of the MASSLF method that require synchronization of the pulse sequence[3,4] with the magic angle spinning are impractical at 77 K using our probehead[1a] because the spin rate can sometimes fluctuate ±100 Hz when liquid N_2 contacts the rotating sample. In this application an alternative sequence[6] has been used which does not require synchronous operation and conveniently provides the dipolar spectral width needed to observe MASSLF patterns for methylenes.

The equipment and technique used for ^{13}C CPMAS matrix isolation NMR has been described elsewhere.[1a] In the 2D MASSLF experiment 200 points in t_1 were acquired with 40 scans per point. For NMR experiments the azo precursor **2a** was synthesized di-^{13}C (>98% isotopic enrichment) from the 3,4-dimethyl 3,4-thiophenedicarboxylate by the same method used previously for **2b**.[1a] The diester was prepared using dimethyl acetylenedicarboxylate-di-$^{13}CO_2Me$[1a,7] and trimethylsilylmethyl

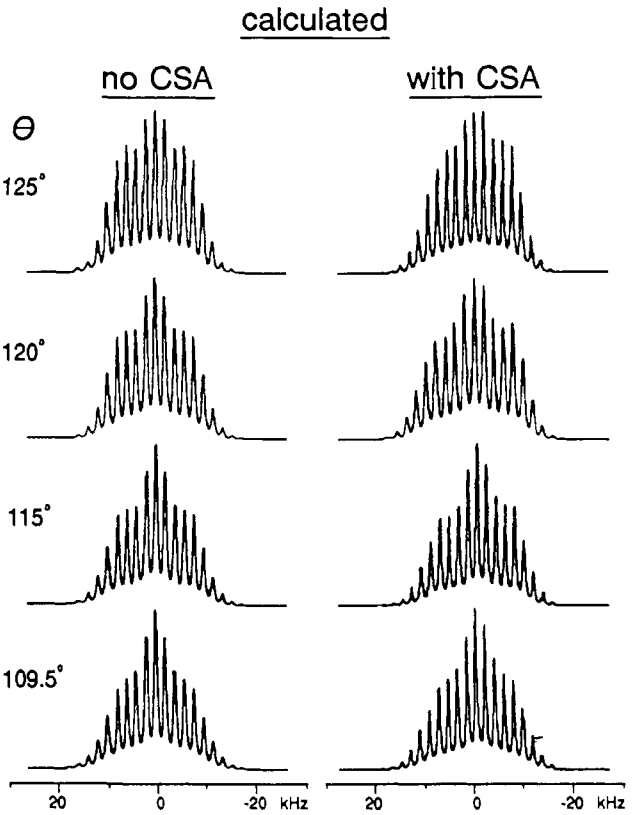

Figure 2. Comparison of MASSLF patterns for CH_2 groups with various H–C–H angles. As the H–C–H angle is widened the outer sidebands rise rapidly in intensity. Note that the change in the outer sideband intensities is more rapid as the angle increases above 120° than when it is made less than 120°. When a CSA is included, the patterns lose their symmetry about the centerband. The CSA used is that described in Figure 1, and r_{CH} was set to 1.08 Å.

chloromethylsulfide[8] followed by iodosobenzene oxidation.[9] The matrix isolation NMR spectra in 2-methyltetrahydrofuran (2-MTHF) before photolysis, after photolysis, and after annealing gave very similar results to those reported earlier[1a] for **1b** and **2b**. An isotropic shift of 105 ppm from tetramethylsilane was observed for the biradical centers in **1a** which is quite close to the 100 ppm shift observed for those in **1b**.

Spectroscopic assignment of the 105 ppm resonance is provided by the MASSLF pattern in Figure 1B. In general, rapidly rotating methyl groups and nonprotonated carbons give MASSLF patterns with only a few weak sidebands.[3,6] Methines produce patterns reminiscent of the Pake doublet line shape, and methylenes give a characteristic tent-shaped pattern[6,10] approximately $\sqrt{2}$ times as wide. Experimental MASSLF patterns for the latter two types of carbon in 2-MTHF are shown in the left of Figure 1 (parts C and D). Comparison of these two patterns with that for the 105 ppm peak in **1a** clearly shows that this resonance is for a methylene group.

While the experimental patterns in Figure 1 (parts B and C) are similar, the relative intensities of the sidebands are noticeably different. The computer simulations[11] to the right of Figure 1, which are essentially identical with the experimental patterns, show that this difference can be fully accounted for by allowing the biradical centers to assume sp^2 geometry. In Figure 2 are computer simulations of CH_2 MASSLF patterns for several H–C–H angles θ. These patterns show that as θ is opened up the outer

(6) (a) Zilm, K. W.; Webb, G. G. *J. Am. Chem. Soc.*, in press. (b) Zilm, K. W.; Webb, G. *Fuel* **1986**, *67*, 707–714.
(7) Huang, S.; Beale, J. M.; Keller, P. J.; Floss, H. G. *J. Am. Chem. Soc.* **1986**, *108*, 1100–1101.
(8) Hosomi, A.; Matsuyama, Y.; Sakurai, H. *J. Chem. Soc., Chem. Commun.* **1986**, 1073–1074.
(9) Takaya, T.; Hijikata, S.; Imoto, E. *Bull. Chem. Soc. Jpn.* **1968**, *41*, 2532–2534.
(10) Herzfeld, J.; Roberts, J. E.; Griffin, R. G. *J. Chem. Phys.* **1987**, *86*, 597–602.
(11) Herzfeld, J.; Berger, A. E. *J. Chem. Phys.* **1980**, *73*, 6021–6030.

sidebands become progressively more intense. In order to achieve close agreement with the experimental MASSLF pattern the chemical shift anisotropy (CSA) must be included. At the relatively low field strength used here (2.35 T), the principal effect of the CSA is to introduce asymmetry about the centerband as shown on the right of Figure 2. Fortunately the full CSA tensor need not be precisely known. For the 2-MTHF methine many essentially identical fits can be found as long as the span of the CSA is approximately 3200 Hz, and the C–H vector is within 35° of perpendicular to the most high field tensor component. The extremely good fit of the experimental biradical MASSLF pattern in Figure 1B was the result of dozens of simulations. These calculations indicate that the difference between the highest field and lowest field CSA components can be no more than 3000 Hz (119 ppm) and no less than 2000 Hz (79 ppm). The best fits with the larger CSA require an r_{CH} of 1.08 Å; for the smaller CSA an r_{CH} of 1.07 Å provides the best agreement. The variation in the MASSLF pattern as the H–C–H angle is opened up for the larger CSA is shown to the right of Figure 2. In all of the cases investigated the H–C–H angle is required to be close to 120°. No reasonable fits can be found once θ becomes larger than 122.5° or smaller than 115° as judged on the basis of the sum of the squares of the deviations in sideband intensities.

The absence of a contact shift in either **1a** or **1b** rules out a triplet ground state for both as argued previously.[1] This fact, in conjunction with the determination of the H–C–H angle in **1a** as 120° and the observation of a CSA half that found in alkenes, provides compelling evidence for the formulation of both species as singlet biradicals.

It should be noted that an effective homonuclear decoupling scaling factor has been determined by fitting the experimental patterns for the 2-MTHF glass assuming that all the C–H distances are 1.09 Å. Other workers[4] have shown that this approach largely corrects for motional averaging by high frequency vibrations and lattice motions. The C–H distances so derived are then relative to the choice of r_{CH} for the 2-MTHF centers. Large amplitude motions are probably not important here as even the rotation of the 2-MTHF methyl group is slowed sufficiently to display dipolar couplings at 77 K. The sidebands in this MASSLF pattern are not resolved, which indicates that the methyl rotation rate is on the order of the dipolar couplings or the MAS spin rate. This is consistent with the value of 3.6 kcal mol^{-1} reported[12] for this barrier. The barrier to rotation for the methylenes in **1a** must be somewhat higher than this as their MASSLF pattern shows no indications of such motional averaging.

In conclusion it has been demonstrated that 2D MASSLF methods in combination with matrix isolation NMR techniques can be used to accurately measure bond lengths and bond angles in captive intermediates. The method also provides for spectroscopic assignment of ^{13}C CPMAS matrix isolation spectra. Use of higher field strengths and lower temperatures in principle should extend the method to natural abundance samples and to species isolated in rare gas matrices.

Acknowledgment. We gratefully acknowledge the support of the National Science Foundation under Grants CHE-8517584 and CHE-8506590. Partial support of this work was also provided by a Grant for Newly Appointed Young Faculty in Chemistry from the Camille and Henry Dreyfus Foundation Inc.

(12) Durig, J. R.; Kizer, K. L.; Karriker, J. M. *J. Raman Spectrosc.* **1973**, *1*, 17–45.

Computer Software Reviews

SlideWrite Plus. Version 2.1. Advanced Graphics Software Inc.: 333 West Maude Avenue, No. 105, Sunnyvale, CA 94086. (408) 749-8620. List price: SlideWrite Plus 2.1 $345.00, Fonts & Figures, $99.00.

SlideWrite Plus is a graphics software package for any 100% IBM compatible personal computer from the PC to the PS/2. This package enables one to create assorted types of graphs (bar, pie, line, scatter) and augment them with curve fits (linear, exponential, polynomial, and others), textual annotations, and clip-art figures. As the name suggests, SlideWrite files can be used to produce slides using the HP 7510, the ImageMaker, or the Polaroid Palette Plus. It also will produce NAPLPS files (with certain size limitations) for use with General Parametrics VideoShow, ColorMetric board, and PhotoMetric camera. To run Slidewrite Plus one must have at least 390 KB of free memory, 2 disk drives or a hard disk, DOS 2.0 (or later), a graphics adapter (AT&T 6300, Hercules Graphics Card, IBM 3270 APA Card, IBM Color/Graphics, EGA, or VGA), and the appropriate monitor. In addition it is very useful to have a mouse. The output can be sent to the screen, a dot matrix or laser printer (1 MB of memory required for full-sized plots), a plotter, or a camera. In testing SlideWrite Plus I used a PC's Limited 286 PC with an EGA card, a Mitsubishi color monitor, and a Logitech mouse. The output was sent to an IBM Proprinter, HP LaserJet+ printer, and an HP 7550 plotter.

Two impressive qualities of SlideWrite Plus are the ease with which one can produce good-looking graphs and the presence of features important to scientists and engineers. Graphs are created by following a logical series of options presented in menu form. The numerical data can be entered either from the keyboard or imported from an ASCII file. (In addition, Lotus 1-2-3 graphs can be imported.) The format of the ASCII data file must be a series of columns with the x values in the first column and the y values for each curve to be plotted in the following columns. SlideWrite Plus can handle up to 4000 pieces of data per graph. For displaying multiple data sets there are six line patterns and twelve symbol types.

SlideWrite Plus has several features of particular interest to the scientist. Either or both axes can be set to log scale. Data can be plotted against a second y axis along the right side of the graph. A second x axis can be displayed along the top of the graph but data cannot be plotted against it. Error bars can be added to four graphs using the other four data sets available for the size of the error bars. There is a provision to annotate graphs with multiple super and subscripts. SlideWrite Plus also contains a very easy to use curve fitting feature. Fits of data may be linear, exponential, log, power, or polynomial. The order of the polynomial fit can be as high as six. In addition to plotting the fit along with the data SlideWrite Plus provides a statistics page for each fit which includes statistical parameters such as the average, standard deviation, coefficients of the polynomials, and the R value of the fit.

In addition to the construction of graphs SlideWrite Plus has a draw mode in which pictures may be added to the final product. In the draw mode one can add lines, boxes, circles, arrows, text, and clip-art figures from the figure library. The introduction of these graphical annotations is controlled by the position of the cursor and a menu along the bottom of the screen. While one can do limited line, circle and box drawing, SlideWrite Plus is not for freehand drawing. Any figure that is more than a straight line, arrow, box, or circle must be imported as a clip-art figure. SlideWrite Plus comes with about 110 figures. None of the figures in the library looks to be of any use to the chemist (see comments on Figures and Fonts).

SlideWrite Plus has several convenient features for displaying or printing multiple graphs. Up to four graphs can be displayed on one page. There is also a batch print feature which allows one to print out 45 graphs with one command.

The Fonts&Figures accessory consists of ten more fonts, a library of about 300 figures, and a figure maker utility. Of the new fonts seven are improved variations of the original fonts and three (two script fonts and a gothic font) are all new. One of the nice improvements made over the original modern bold and modern light fonts is the entire Greek alphabet. Of the 300 new figures in Fonts&Figures there are eighty in the "chemistry library". Most of these figures are simple chemical structures. Fifty of the figures in the chemistry library are five- or six-membered rings with various options for heteroatoms. The most complex structure